ACCESS
Arctic Climate Change
Economy and Society

Project no. 265863

ACCESS

Arctic Climate Change, Economy and Society

Instrument: Collaborative Project

Thematic Priority: Ocean.2010-1 “Quantification of climate change impacts on economic sectors in the Arctic”

D2.41 – Air pollution and surface deposition related to present and future Arctic shipping

Due date of deliverable: **28/02/2015**

Actual submission date: **17/03/2015**

Start date of project: **March 1st, 2011** Duration: **48 months**

Organisation name of lead contractor for this deliverable: **DLR**

Project co-funded by the European Commission within the Seventh Framework Programme (2007-2013)		
Dissemination Level		
PU	Public	
PP	Restricted to other programme participants (including the Commission Services)	
RE	Restricted to a group specified by the consortium (including the Commission Services)	
CO	Confidential, only for members of the consortium (including the Commission Services)	X

Contents

Contributing Authors:

Anke Roiger[1], Jennie L. Thomas[2], Louis Marelle[2], Jean-Christophe Raut[2], Bernadett Weinzierl[1,3], Jin Kim[1], Anja Reiter[1], Stig Dalsøren[4], Kathy S. Law[2] and Hans Schlager[1]

Lead PIs: Kathy S. Law[2] and Hans Schlager[1]

[1] Deutsches Zentrum für Luft- und Raumfahrt (DLR), Institut für Physik der Atmosphäre, Oberpfaffenhofen

[2] Sorbonne Universités, UPMC Univ. Paris 06; Université Versailles St-Quentin; CNRS/INSU, LATMOS-IPSL, Paris, France

[3] Ludwig Maximilians Universität (LMU), Meteorologisches Institut, 80333 München, Germany

4 Center for International Climate and Environmental Research-Oslo (CICERO), Oslo, Norway.

1. Introduction and task description

Arctic sea ice has decreased dramatically in the past few decades and the Arctic is increasingly open to shipping. Transit shipping through the Arctic as an alternative to the traditional shipping routes is currently underway. These activities are expected to increase emissions of air pollutants and climate forcers (e.g. aerosols, ozone) in the Arctic troposphere significantly in the future. However, large knowledge gaps exist regarding composition and impacts of associated emissions.

The overall objective of task 2.41 "Pollution in the Arctic from Arctic shipping" is to quantify the impact of different types of shipping on Arctic air quality and regional climate by using a combination of measurements and modelling. Section 2 summarizes the results from in-situ measurements and data analysis of the ACCESS aircraft campaign (Roiger et al., 2014). Using the ACCESS measurements, a modelling study was performed to study local and regional scale effects of Arctic shipping with a focus on northern Norway, discussed in section 3 (Marelle et al., 2015). Finally, the results from a global modelling study of the environmental impact of shipping emissions are presented in section 4, with a special focus on the Arctic region (Dalsøren et al., 2013).

2. In-situ measurements of Arctic shipping emissions during the ACCESS aircraft campaign 2012

The ACCESS campaign focused on the impact of Arctic climate change including human activities in the Arctic. During the ACCESS aircraft campaign 14 flights were performed. Nine flights were dedicated to studying Arctic air pollution, with 5 flights during which shipping emissions of several vessel types using different types of fuel were sampled. In-situ observations included measurements of carbon monoxide (CO), ozone (O_3), nitrogen monoxide (NO), nitrogen dioxide (NO_2), nitric acid (HNO_3), sulfur dioxide (SO_2), aerosol number concentration and size distribution, refractory black carbon (rBC) mass and number concentration, as well as a suite of meteorological observations. Most of the measurements

were performed at a high temporal resolution of typically 1 second corresponding to a spatial resolution of about 100 to 200 m (depending on flight altitude).

There are a number of publications on in-situ measurements of emissions from various vessel types and under different conditions (Hobbs et al., 2000; Lack et al., 2009; Lack et al., 2011; Lack et al., 2012; Williams et al., 2009; Jonsson et al., 2011; Diesch et al., 2013; Cappa et al., 2014; Beecken et al., 2014). During ACCESS we generally focused on the smaller vessel types, which are expected to operate in the Arctic in the future. We sampled fresh emissions released by different types of ships, including cargo, passenger ships and fishing vessels using different fuels including Heavy Fuel Oil (HFO) and Marine Gas Oil (MGO). MGO is more refined than HFO and has lower sulfur content. Table 1 lists all vessels we probed, including vessel types, dimensions, and engine type. It also shows ratios of observed emissions, namely ratios of SO_2 (which is dependent on fuel sulfur content) to NO_x (which is related to combustion temperatures) and the fraction of non-volatile particles. The plumes were usually sampled very close to the ships to prevent any atmospheric processing. It is worth noting that sampling of emissions close to fishing boats was complicated by the large number of birds around the vessels, and the resulting safety issue for the aircraft. As expected, the lowest SO_2/NO_x ratio was observed for the ship running with MGO (Wilson Leer), while the highest ratio was found in the plume released by the largest vessel (Costa Deliziosa). The percentage of non-volatile particles by number ranged between 50 and 79%, similar to findings of Petzold et al. (2008) and Moldanová et al. (2013).

Table 1. Summary of ship emission measurements

Flight number	Name of Vessel	Vessel Type	Gross Tonnages / Dimensions	Engine type	SO_2/NO_x [a] (No. of plume samples)	Fraction (by number) of non-volatile particles [a] (No. of plume samples)
#1	Costa Deliziosa	Passenger ship	92720	Medium speed diesel engine	0.57 ± 0.14 (7)	0.79 ± 0.11 (7)
#9	Mikhail Strekalovski	Bulk carrier	16253	Slow speed diesel engine	0.44 ± 0.11 (2)	0.50 ± 0.07 (2)
#2	Wilson Nanjing	Cargo ship	6118 [b]	Medium speed diesel engine	0.47 ± 0.12(6)	0.65 ± 0.09 (5)
#1	Wilson Leer	Cargo ship	2446 [c]	Medium speed diesel engine	0.05 ± 0.01 (1)	n/a [e]
#9	Koralen	Fishing boat	LxB [d] = 49x9m	unknown	0.13 ± 0.03 (2)	0.75 ± 0.11 (4)
#9	Sorvik	Fishing boat	LxB [d] = 15x6m	Medium speed diesel engine	0.15 ± 0.04 (1)	0.69 ± 0.10 (1)

a) The ratios of SO_2/NO_x and the fraction of non-volatile particles were calculated using the integrated peak areas for each plume encounter. Uncertainties were calculated using the instrument uncertainties combined in quadrature.

b) Fuel Type: RMG380CST

c) Fuel Type: Marine gas oil (DMA), sulfur content 0.082

d) LxB: Length x Beam (width at the widest point) in meters

e) The dilution system was switched off during this plume measurement and the total particle number concentrations exceeded the upper detection limit of the instrument

During the ACCESS flights on 11, 12 and 25 July, we also investigated the chemical and dynamical evolution of pollutants released by different vessel types (small and mid-size cargo ships, passenger vessels), similar to the studies of e.g. Song et al. (2003), Chen et al. (2005) and Petzold et al. (2008). Figure 1 exemplary illustrates the performance of such a single plume study. On 12 July, the Wilson Nanjing, a mid-size cargo ship running with HFO, travelled northward along the Norwegian Coast. The northerly wind conditions on that day resulted in the heading of the ship being into the wind, resulting in rapid dilution of the plume. Plume dispersion forecasts from the HYSPLIT model were used to plan this experiment and the Falcon flight was designed to cover the 3 dimensional structure of the evolving plume, from the vicinity of the vessel up to a downwind distance of more than 70 km. The flight was performed in close collaboration with the ship operator (Wilson Ship Management). On the day of the experiment, the captain reported his current position, vessel speed, and heading, which allowed the calculation of the approximate plume position at the time of the flight. HYSPLIT plume forecasts were performed using emission tracers released every minute along the planned ship track (Fig. 1a).

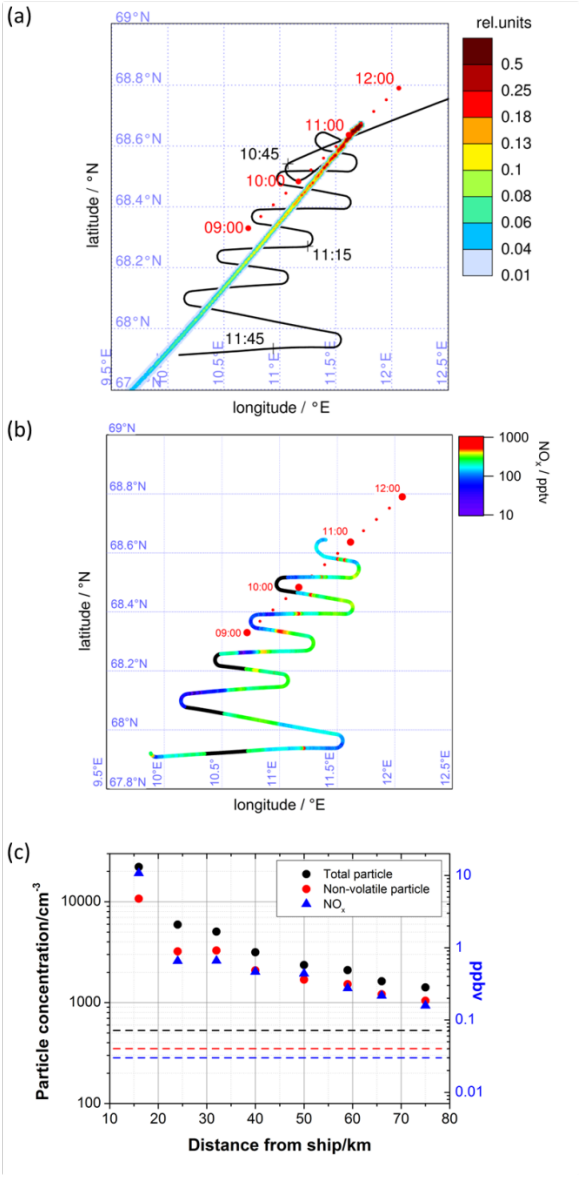

Fig. 1. (a) HYSPLIT forecast of the Wilson Nanjing plume location at the altitude of the aircraft measurements. HYSPLIT run was initialized using the ECMWF meteorology forecast (11 July, 12:00 UTC). (b) Flight track of the single plume study on 12 July (~10:50h – 11:50h UTC), color-coded by measured NO_x concentration. Black color indicates missing data due to internal calibration periods. (c) Measured maximum concentrations of total particle number (black), non-volatile particle number (red), and NO_x (blue) as a function of distance from the Wilson Nanjing. Instrument uncertainties are 15% for NO_x and 10% for total and non-volatile particles. The dashed lines represent corresponding background concentrations. Taken from Roiger et al., 2014.

Fig. 1b shows the measured NO concentration along the flight path on 12 July 2012. At the beginning of the flight, the Falcon approached the vessel to search for the fresh plume, indicated by strong enhancements in gas and aerosol concentrations (as observed by the instrument operators onboard the Falcon). The plume was then sampled downstream during several passes, based on the positions as forecast by the HYSPLIT model in combination with real-time in-situ measured wind direction. Communication between the pilots, the mission scientist and the instrument operators ensured that the plume was encountered during each transect, before the Falcon proceeded to the next flight leg. The slight gradient in observed NO mixing ratios towards the coast may have been due to other ships travelling in the measurement region. The maximum NO_x, total and non-volatile particle concentrations measured during each plume transect is presented as a function of distance from the emission source in Fig. 1c. It shows that aerosol and NO_x concentrations were still above background levels even ~1.5 hours after emission.

3. Local and regional scale modelling of current Arctic shipping emissions with a focus on northern Norway

This section summarizes results from local and regional modelling of shipping emissions along the Norwegian Coast. The current impact of shipping along the Norwegian coast in July 2012 is estimated using the STEAMv2 emission inventory in combination with the FLEXPART-WRF and the WRF-Chem model (see next sub-section). The derived emissions estimates also are compared with the results from the ACCESS in-situ measurements.

Methods and Tools

The study makes use of the STEAMv2 emission inventory (Jalkanen et al., 2012) as well as of the plume dispersion model FLEXPART-WRF and the WRF-Chem model 3D chemical transport WRF-Chem (Weather Research and Forecasting model, including chemistry, Grell et al., 2005), which are described shortly in the following. For more details, see Marelle et al. (2015). **FLEXPART-WRF** (Brioude et al., 2013) is a version of the Lagrangian particle

dispersion model FLEXPART, driven by meteorological fields from the mesoscale weather model WRF (Weather Research and Forecastin). FLEXPART-WRF is run with WRF version 3.5.1 meteorological simulations from 4 to 25 July 2012, over the domain presented on Figure 2a. This domain, at 15 x 15 km horizontal resolution, covers most of Northern Norway and all the ACCESS ship flights. Moving ship emissions are represented in the FLEXPART-WRF plume dispersion simulations as fixed box sources, emitting successively along the ship route (shown on Fig. 2b). The ship tracks were divided in 1000 such sources approximately 100 m x 100 m x 5 m wide, but whose size depends on ship speed and course. Those box sources emit a constant flux of air tracer. Ship emissions injection heights are calculated with a simple plume rise model (Briggs, 1965).

In order to estimate shipping impacts in Northern Norway, simulations are performed using the 3D chemical transport **WRF-Chem** (Weather Research and Forecasting model, including chemistry, Grell et al., 2005). WRF-Chem simulations are performed on the same 15 x 15 km domain presented on Figure 2a.

Ship emissions used in the WRF-Chem simulations are generated by the high resolution, real time shipping inventory **STEAMv2** (Jalkanen et al., 2012). STEAM v2 generates ship emissions using activity data from a ship tracking system, the Automatic Identification System (AIS). STEAMv2 calculates each ship's fuel consumption based on its speed, engine type, fuel type, vessel length and propeller type. The model also takes into account the effect of waves, and distinguishes ships at berth, maneuvering ships and cruising ships.

Results from local modelling

Figure 2 shows the location of 5 ACCESS flights focused on local Arctic emissions, on 11, 12, 19 and 25 July 2012. Flights on 11, 12 and 25 July 2012 were single-plume flights, during which the research aircraft sampled the emissions of specific ships, relatively close to the source (< 80 km, see also section 2). Measurements from these single plume flights are used in this study to estimate emissions from the targeted ships. The method used here relies on knowing the precise locations of the ships during sampling, Because those locations are not

available for the 25 July 2012 flight, emissions are only estimated for the 3 ships targeted during the 11 and 12 July flights. Information about these 3 ships is shown in Table 1.

The 19 July 2012 flight was not focused on specific ship sources, but included low altitude parts in the marine boundary layer near Trondheim, where aged ship emissions were likely to be sampled. All the flights presented on figure 2 are thus used herein to validate regional chemical transport simulations investigating the impacts of shipping in Northern Norway.

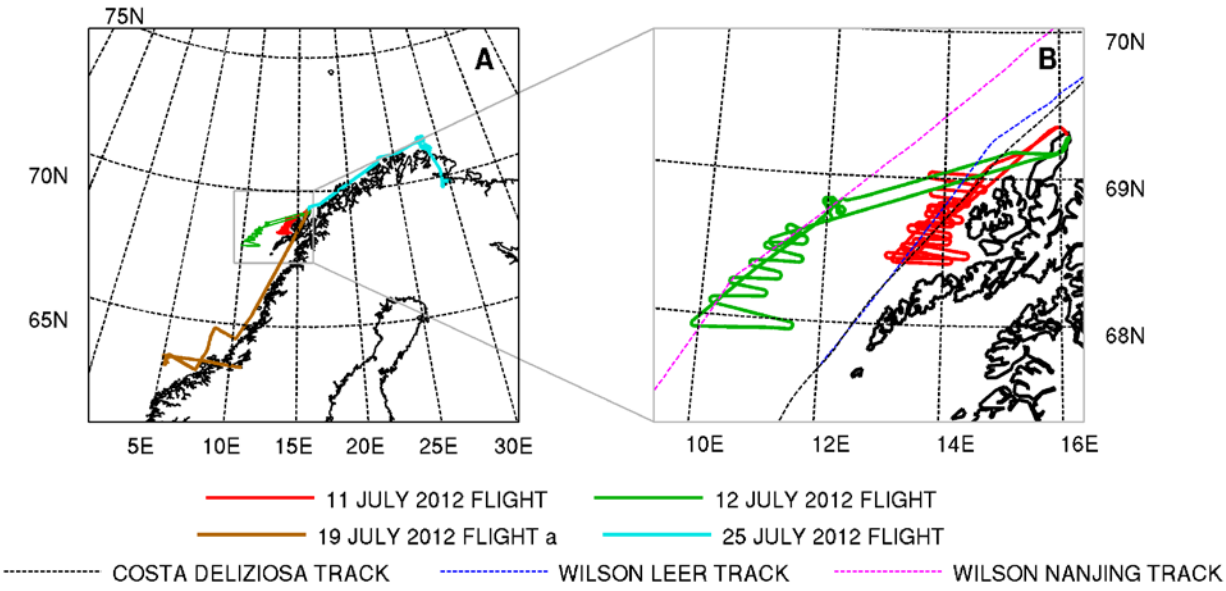

Figure 2. (a) 15 x 15 km resolution WRF and WRF-Chem domain, with ACCESS flight tracks during the 11, 12, 19 (flight a) and 25 July 2012 flights, (b) 3 x 3 km resolution WRF domain, with the tracks of the 3 ships targeted during the 11 and 12 July 2012 flights.

FLEXPART-WRF plume dispersion simulations were performed for each of the 3 ships targeted during ACCESS. Figure 3 shows the comparison between airborne measurements of NOX and FLEXPART plume location for the Wilson Leer and Costa Deliziosa during the first half of the 11 July 2012 flight. This figure shows the typical meandering pattern of the plane during ACCESS, measuring the same ship plumes several times as they aged, further and further away from the ship. Figure 3 also illustrates the good agreement between modeled and measured plume locations for both ships.

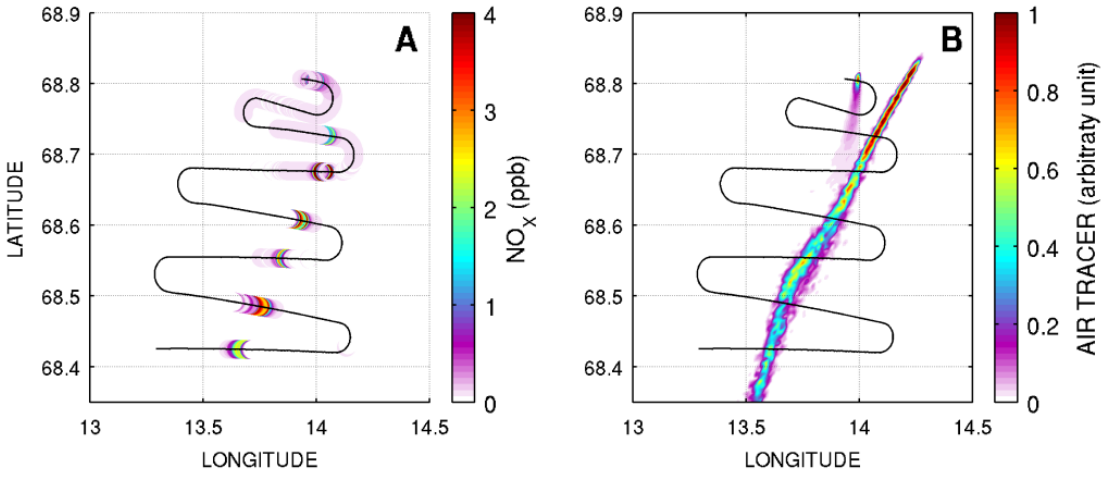

*Figure 3. (**a**) ACCESS NO_X measurements between 16:00 and 16:35, 11 July 2012 (Z ~ 49 m). (**b**) ACCESS flight track (black) and FLEXPART WRF air tracer mixing ratios at Z = 45 m for the Wilson Leer and the Costa Deliziosa. FLEXPART plumes are represented at the approximate average time of sampling: 16:00 for the Wilson Leer (above and left on panel B) and 16:18 for the Costa Deliziosa (below and right). FLEXPART results are normalized using the peak tracer concentration at Z=45 m.*

Results from regional modelling

Regional scale impacts of ships in Northern Norway are estimated by calculating the 15-day average difference between the CTL and NOSHIPS simulation. Figure 4 shows maps of these anomalies at the surface, for BC, O3 and PM2.5. Ship emissions have the largest influence on surface BC concentrations with a 25 to 50 % increase of concentrations along the coast. As expected, absolute values at the highest in the southern part of the domain, where ship emissions are the highest. However, those BC emissions do not seem to be efficiently transported inland. Average O3 increases from shipping are 6 to 7 % (~ 2 ppb) in the coastal regions, but also further inland into Sweden. The impact of ships on O3 is more significant if we only consider the effects at local noon instead of the day and night average shown of Figure 4 and can reach 3 ppb, (10 %).

The impact of Norwegian ships on summer surface ozone has been investigated by Dalsøren et al. (2007). They found, for July 2000, a 1 to 1.5 % increase in O3 from Norwegian ships along the coast and in Norway and Sweden. This earlier study also included projections for 2015 of the combined effects of increased Norwegian coastal shipping, increased international traffic, traffic associated with oil and gas extraction, and transit by the Northern Sea route, along with increased emissions from coastal power generation. Those projections predicted a further ~ 6 % increase in surface ozone in the region, values comparable with the 2012 increases from the present study from Norwegian shipping only. This means that current increases in surface ozone due to Norwegian shipping are likely to be higher than earlier projections.

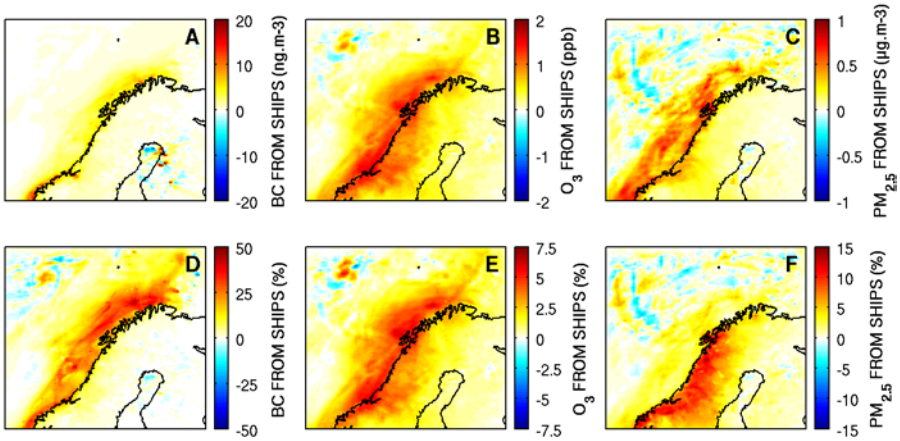

Figure 4. 15-day average (11-26 July 2012) of (top) absolute and (bottom) relative surface enhancements in ***(a, d)*** *BC,* ***(b, e)*** *O_3 and* ***(c, f)*** *$PM_{2.5}$ due to Norwegian ship emissions.*

4. Global modeling of the environmental impact of shipping in 2030 with a focus on the Arctic region

This section presents results from a global modelling study described in detail in Dalsøren et al. (2013). The study analyses the impact of changes in shipping emissions from 2004 to 2030 using the chemistry transport model OsloCTM2. For more details of the model set-up, see Dalsøren et al. (2013). The emission data sets are taken from Corbett et al. (2010) who provides gridded inventories for current (2004) and future (2030) ship emissions of greenhouse gases and gas and particulate pollutants in the Arctic. Two scenarios are used for 2030. In the high growth scenario (HIGH), there is more than doubling in energy use from 2004 to 2030 for shipping serving in the Arctic, and 2% of the global traffic is diverted through the Arctic. Global shipping growth outside the Arctic is + 3.3 % per year on average, and most uncontrolled emissions grow proportionally to shipping activity. For some pollutants there are exceptions; SOx and NOx follow new global IMO regulations to be implemented by 2020 and OC is correlated with changes in SOx emissions. Compared to the Arctic ship emission inventory for 2004, large emission increases (factors of 2 to 5) are found for all species except sulfur where regulations on sulfur content outweigh the increase in

fuel consumption. In 2030, the emissions from diversion traffic are larger than those from the fleet operating solely within the Arctic.

The MFR (maximum feasible reduction) scenario for 2030 assumes a business as usual scenario with a maximum feasible reduction in black carbon emissions. 1 % of the global traffic diverts to Arctic through-routes, and global shipping growth outside the Arctic is + 2.1 % per year. SO_x and NO_x reductions follow IMO regulations and OC is correlated with SO_x, unless additionally reduced by MFR controls. Compared to 2004, NO_x emissions from shipping in the Arctic are doubled, but MFR controls reduce BC by some 70%, sulfur emissions are halved, and OC which is correlated both with sulfur and BC is about one third. With these scenario conditions, yearly total 2030 emissions for regional Arctic traffic in MFR are factors 1.5 to 1.7 larger than for the diversion traffic. To illustrate the large dependency of atmospheric impacts on seasonality in emissions and meteorology results are shown as seasonal means. Average changes from 2004 to 2030 for key air pollutants are presented for the four seasons NDJ (November-December-January), FMA (February-March-April), MJJ (May-June-July) and ASO (August-September-October, i.e., the period with Arctic transit traffic in 2030).

Figure 5 shows the average ASO surface distribution of NO_2 in 2004 as well as absolute changes in 2030 due to the HIGH and MFR ship scenarios. In 2004 the highest NO_2 concentrations are found over industrialized regions, megacities and areas with frequent vegetation fires. In both future scenarios the NO_2 changes are close to or within the shipping lanes, due to the short atmospheric lifetime of this gas. For the MFR scenario increases are typically 10-80 pptv (10-40 % relative to 2004) outside Arctic waters, with larger absolute increases in the highly trafficked English Channel and North Sea. In the Arctic similar perturbations are found in regions with internal Arctic traffic, for instance around Iceland. The diversion routes are more clearly visible, exhibiting increases from 80 to 200 pptv (above 200 % in pristine regions). In the HIGH scenario there are large increases, up to hundreds of pptv, in the Arctic (above 200 %) for the ASO season, but much smaller changes in NDJ when ice conditions prevent trade route diversion and allow less internal traffic. The changes in coastal regions in the Northern Hemisphere are substantial, from 60 to above 200 pptv (20-

60 %). In the Southern Hemisphere the increases in major shipping lanes are typically 20-50 pptv (20-60%).

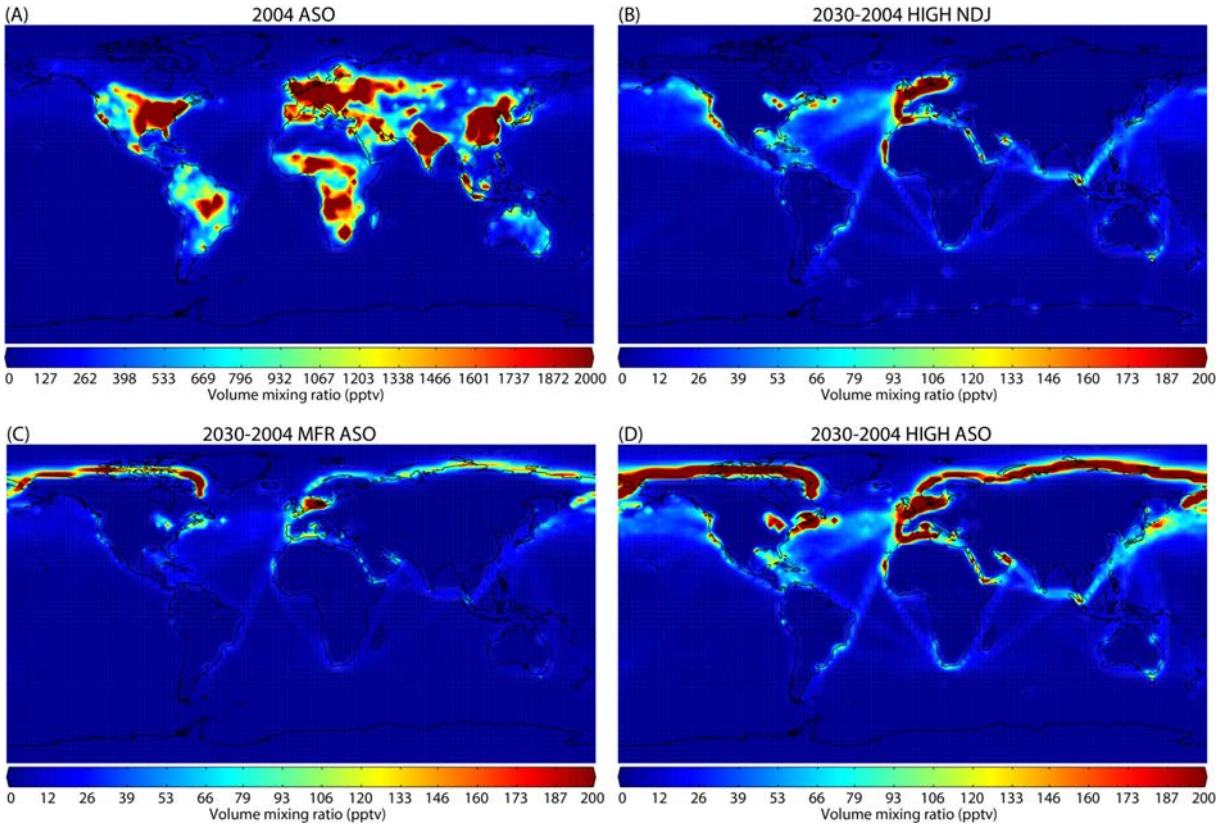

Figure 5: NO_2 in the lowest model layer close to the surface (pptv). **(A)** Average 2004 for the months August-Sept-Oct (ASO). **(B)** Average change 2004-2030 for HIGH scenario for the months November-Dec-Jan (NDJ). **(C)** Same as (B), MFR scenario, months ASO. **(D)** Same as (B), HIGH scenario, months ASO.

The year 2004 ASO and NDJ distributions of surface ozone are shown in Figure 6. High levels are found downwind of polluted regions with extended periods of sunlight and favorable conditions for ozone formation, especially over oceans and deserts where dry deposition is slow. The changes in the MFR scenario are moderate, a few ppbv/percent over the oceans and coastal areas. Except for the ASO season small changes are found in the Arctic region. This is expected since the NO_x emissions from traffic within the Arctic are only slightly larger than in 2004. Since ship emissions of other ozone precursors (VOCs, CO) are small, NO_x ($NO+NO_2$) is decisive for ozone generation from shipping. For the MFR in the ASO season the

effect of diversion traffic on ozone is limited since it occurs (August-October) outside the months with maximum insolation. In September-October the sunlight in the Arctic is rapidly diminishing and ozone formation is getting less efficient. In general substantial increases of 2 to above 5 ppv (4 to above 10 %) are found in the Northern Hemisphere coastal and oceanic regions for the HIGH scenario. Many of the countries in western Europe see ozone increases on the order 3-6 %. In pristine regions of the tropical and Arctic Oceans the increases are above 10 %. In MJJ (not shown) the magnitude and spatial patterns of changes has many similarities to ASO. However, the changes in the Arctic are smaller since diversion traffic is absent, and larger over oceanic areas 30-60° N due to the maximum in photochemical activity.

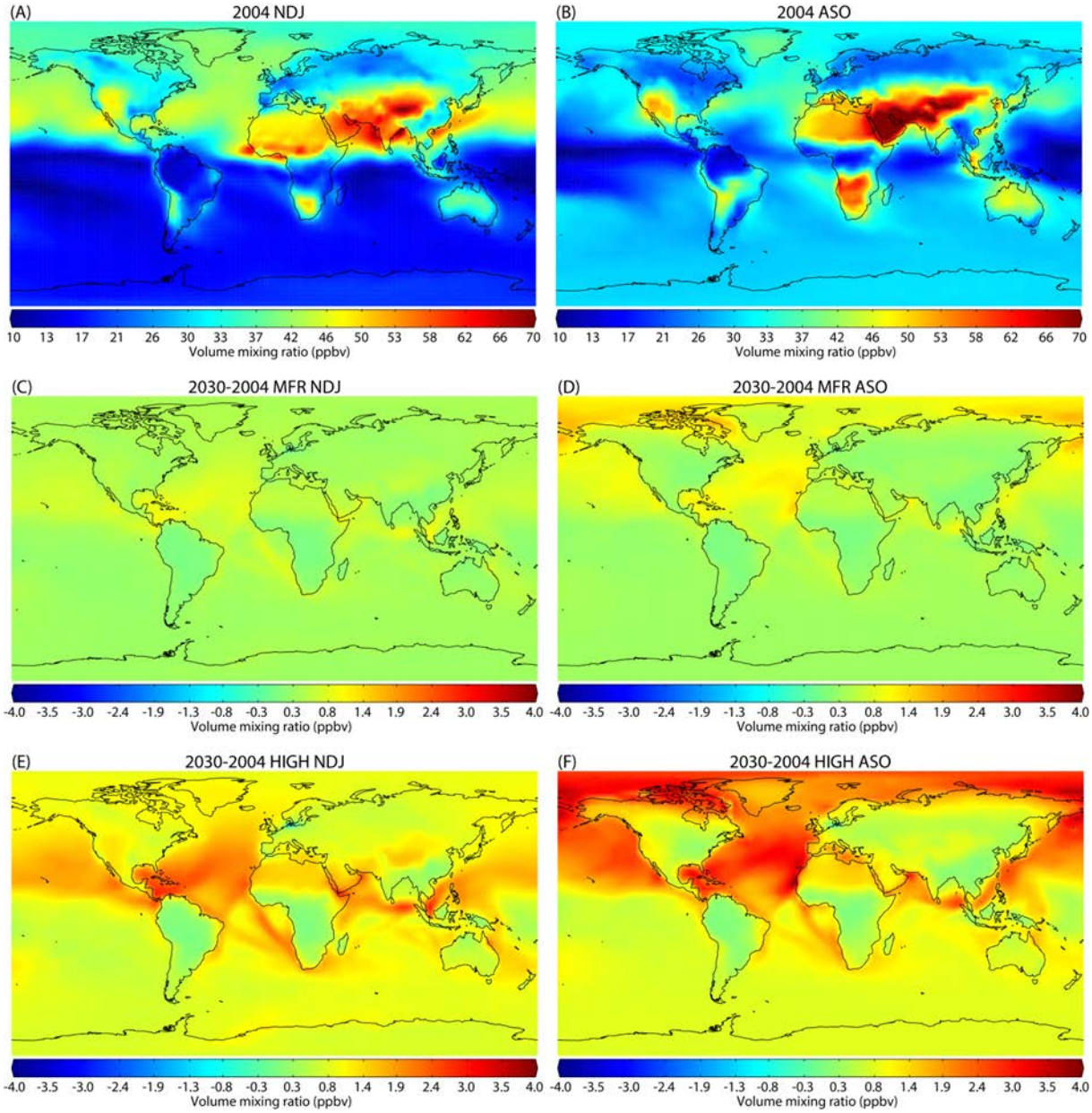

Figure 6: O_3 in the lowest model layer close to the surface (ppbv). Averages 2004 for the months November-Dec-Jan (NDJ) **(A)** and August-Sept-Oct (ASO) **(B)**. Average change 2004-2030 MFR scenario for the months NDJ **(C)** and ASO **(D)**. Average Change 2004-2030 HIGH scenario for the months NDJ **(E)** and ASO **(F)**.

The highest sulfate levels are found close to land-based sources such as industry and power plants in regions with high coal consumption (Figure 7). The maximum concentrations are found in Asia. High sulfate levels are also found in regions with volcanic activity. Figure 7 shows that if the IMO regulations are applied successfully, future reductions are expected at

mid-latitudes. The reductions are however smaller than the decrease of sulfur emissions. This is because most sulfur is emitted as SO_2, and increases in oxidants (OH, O_3 and H_2O_2) lead to more efficient sulfate formation. On the west coast of the continents with prevailing westerly winds, a reduction of around 50 pptv or 10-15 % is clearly of significance, both with regard to health impact from particle pollution and acid precipitation. An increase of up to 50 % is found for the ASO season for the HIGH scenario in proximity to the new diversion routes. This is expected as there are few other large sources of sulfur emissions close to these routes.

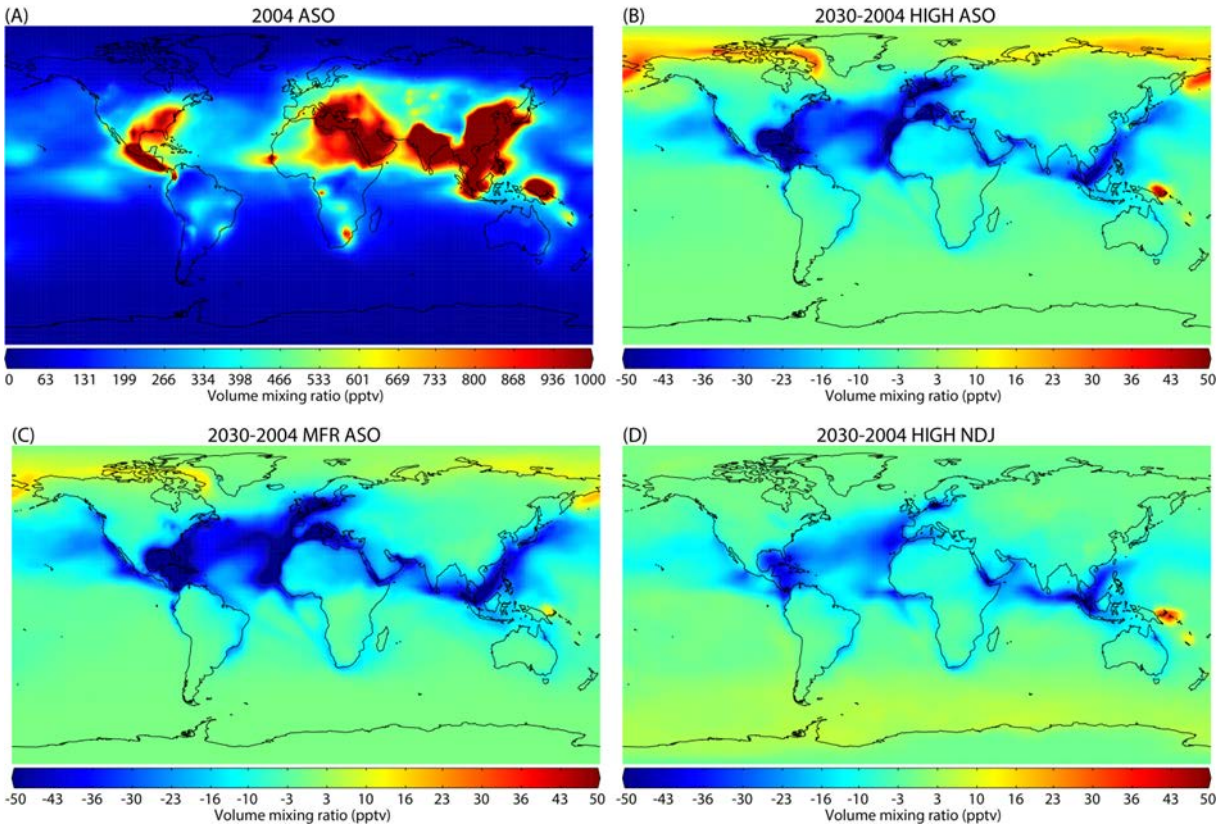

Figure 8: Sulfate in the lowest model layer close to the surface (pptv). (A) Average 2004 for the months August-Sept-Oct (ASO). (B) Average change 2004-2030 HIGH scenario for the months ASO. (C) Same as (B), MFR scenario (D) Same as (B), HIGH scenario, months November-December-January (NDJ).

The highest surface concentrations of black carbon (BC) are found in China and India where biofuel use in households is common (Figure 8). High levels are also found in other densely

populated regions, megacities and areas with vegetation burning. Outside the Arctic future shipping leads to increased BC in the vicinity of major shipping routes. Typical increases are 3-20 ng/m^3 (10-20 %) for the HIGH case, and somewhat lower for the MFR scenario. The largest absolute perturbations are found in the North Sea and other regions with much traffic. However, the largest relative increases are found in the less trafficked area near Antarctica due to the very low background values there. For the MFR scenario in the ASO season the Arctic has a decrease of about 10 % in regions with internal traffic, and a similar or larger increase in the regions with diversion traffic. For the HIGH scenario, which has no measures on BC emissions, the situation is different. There is an increase in the whole of Arctic (Figure 8), and the signals along the diversion routes are very evident. The BC levels increase more than 50 % in much of the Arctic. Arctic changes are smallest in NDJ in both scenarios, mainly due to less traffic and emissions in winter.

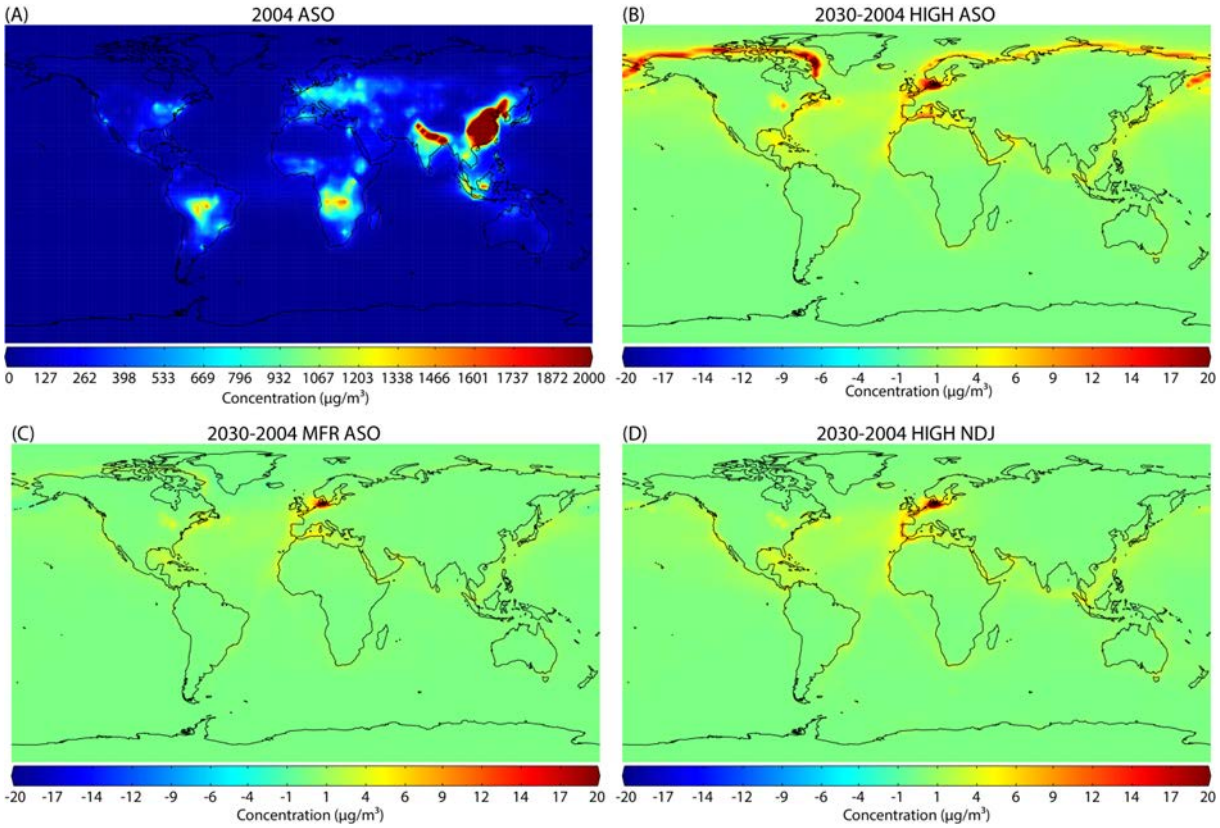

Figure 8: Same as Figure 7 for BC (µg/m^3).

The surface distribution of OC (Figure 9) for 2004 shows many of the same source signatures as BC, but with a stronger signal around regions with vegetation fires. From 2004-2030 OC

concentrations due to shipping decline in most regions, since OC emissions are correlated with SO_x emissions and sulfur content is reduced following IMO regulations. Reductions are typically 4-20 ng/m^3 near shipping lanes in the MFR case. This corresponds to a relative reduction of about 5 % both at mid- and polar latitudes. The diversion routes in the ASO season are again an exception, with increases of 10-30 % in the HIGH scenario.

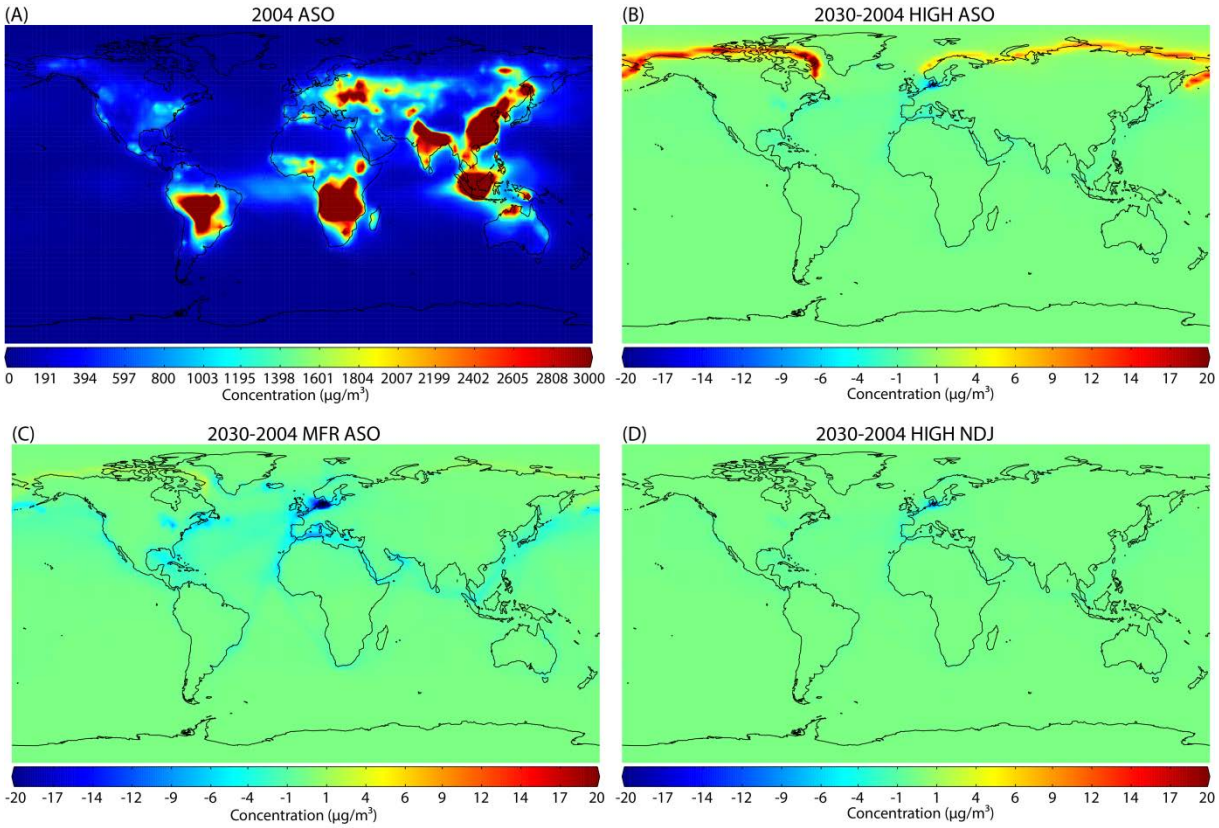

Figure 10: Same as Figure 9 for OC (µg/m^3).

5. Conclusions

ACCESS has provided new independent estimates of emissions from local shipping. Estimates based on aircraft data analysis has been used to validate reported emissions as well as emissions derived from detailed model calculations. Additional sampling of these and other local emissions would provide further constraints on local Arctic emissions especially those that remain highly uncertain (e.g. petroleum extraction, smelting, burning of wood or rubbish).

Arctic shipping emissions are already having significant impacts on local and regional levels of air pollutants, especially in the vicinity of coastal regions.

For future impacts two datasets for ship emissions in 2030 were used that characterize the potential impact from shipping and the degree to which shipping controls may mitigate impacts: A high (HIGH) scenario and a low scenario with Maximum Feasible Reduction (MFR) of black carbon emissions in the Arctic. In the high growth scenario (HIGH) there is a large increase in ship traffic within the Arctic. In addition 2 % of the yearly global traffic diverts to Arctic through-routes during late summer. Global shipping growth outside the Arctic is + 3.3% per year. In the Maximum Feasible Reduction (MFR) scenario a business as usual scenario is followed but maximum feasible reduction is applied on Arctic black carbon emissions. In this scenario, 1 % of the global traffic diverts to Arctic through-routes. Global shipping growth outside the Arctic is + 2.1 % per year. Counteracting the traffic growth in both scenarios is a phase in of existing regulations, resulting in reduced emission factors for some components. The impacts of the scenarios on Arctic and global air pollutant levels were compared to the impacts of current (year 2004) ship emissions using a chemical transport model (Dalsøren et al. 2013). In both future scenarios substantial surface NO2 changes are found close to or within the shipping lanes. Increases from 2004 to 2030 are typically in the range 10 % to above 60 % in coastal regions of the Northern Hemisphere, Arctic shipping regions, and main oceans shipping lanes in both hemispheres. In late summer, when operation takes place along the diversion routes, increases are above 200 % in pristine regions of the Arctic. The largest NO2 changes are found for the HIGH scenario. For surface ozone the HIGH scenario shows substantial increases of 2 to above 5 ppv (4 to above 10 %) in coastal and oceanic regions of the Northern Hemisphere. In pristine regions of the Arctic Oceans the increases are above 10 %. The ozone changes in the MFR scenario are moderate and a few ppbv/percent. For black carbon (BC) in the MFR scenario, the Arctic has a decrease from 2004 to 2030 of about 10 % in regions with internal traffic, and a similar or larger increase in the regions with diversion traffic. For the HIGH scenario, which has no measures on BC emissions, the situation is different. There is an increase in the whole of Arctic, especially along the diversion routes. The BC levels increase more than 50 % in much of the Arctic. Due to regulations, reductions in future sulfate levels are found over the period

2004-2030. On the west coast of the continents at mid latitudes reduction around 50 pptv or 10-15 % is important and could reduce health impact from particle pollution and acid precipitation. Increases (up to 50 %) are only found in regions near the diversion routes in the Arctic in the months of operation (August-October). OC emissions correlate with sulfur emissions and surface OC shows relative reductions of about 5 % both at mid and polar latitudes. The diversion routes in the late summer season are an exception to this, with increases of 10-30 % in the HIGH scenario.

6. References

Beecken, J., Mellqvist, J., Salo, K., Ekholm, J., and Jalkanen, J.-P.: Airborne emission measurements of SO2 , NOx and particles from individual ships using a sniffer technique, Atmos. Meas. Tech., 7, 1957-1968, doi:10.5194/amt-7-1957-2014, 2014.

Brioude, J., Arnold, D., Stohl, A., Cassiani, M., Morton, D., Seibert, P., Angevine, W., Evan, S., Dingwell, A., Fast, J. D., Easter, R. C., Pisso, I., Burkhart, J., and Wotawa, G.: The Lagrangian particle dispersion model FLEXPART-WRF version 3.1, Geosci. Model Dev., 6, 1889-1904, doi:10.5194/gmd-6-1889-2013, 2013.

Cappa, C. D., and Coauthors: A case study into the measurement of ship emissions from plume intercepts of the NOAA ship Miller Freeman. Atmos. Chem. Phys., 14, 1337-1352, doi:10.5194/acp-14-1337-2014, 2014.

Chen, G., and Coauthors: An investigation of the chemistry of ship emission plumes during ITCT 2002, J. Geophys. Res., 110, D10S90, doi:10.1029/2004JD005236, 2005.

Corbett, J. J., Lack, D. A., Winebrake, J. J., Harder, S., Silberman, J. A., and Gold, M.: Arctic shipping emissions inventories and future scenarios, Atmos. Chem. Phys., 10, 9689-9704, doi:10.5194/acp-10-9689-2010, 2010.

Dalsøren, Stig B., Øyvind Endresen, Ivar S. A. Isaksen, Gjermund Gravir and Eirik Sørgård, 2007. Environmental impacts of the expected increase in sea transportation, with a particular focus on oil and gas scenarios for Norway and Northwest Russia.. Journal of Geophysical Research, 112.

Dalsøren, S. B., Samset, B. H., Myhre, G., Corbett, J. J., Minjares, R., Lack, D., and Fuglestvedt, J. S.: Environmental impacts of shipping in 2030 with a particular focus on the Arctic region, Atmos. Chem. Phys., 13, 1941-1955, doi:10.5194/acp-13-1941-2013, 2013.

Diesch, J.-M., Drewnick, F., Klimach, T., and Borrmann, S.: Investigation of gaseous and particulate emissions from various marine vessel types measured on the banks of the Elbe in Northern Germany, Atmos. Chem. Phys., 13, 3603-3618, doi:10.5194/acp-13-3603-2013, 2013.

Grell, G. A., Peckham, S. E., Schmitz, R., McKeen, S. A., Frost, G., Skamarock, W. C., Eder, B.: Fully coupled "online" chemistry within the WRF model, Atmos. Environ., 39, 6957–6976, 2005.

Hobbs, P. V., and Coauthors: Emissions from Ships with respect to Their Effects on Clouds. J. Atmos. Sci., 57, 2570-2590, 2008.

Jalkanen, J.-P., Johansson, L., Kukkonen, J., Brink, A., Kalli, J., and Stipa, T.: Extension of an assessment model of ship traffic exhaust emissions for particulate matter and carbon monoxide, Atmos. Chem. Phys., 12, 2641-2659, doi:10.5194/acp-12-2641-2012, 2012.

Jonsson, Å. M., Westerlund, J., Hallquist, M.: Size-resolved particle emission factors for individual ships. Geophys. Res. Lett., 38, L13809, 2011.

Lack, D. A., and Coauthors: Particulate emissions from commercial shipping: Chemical, physical, and optical properties. J. Geophys. Res.-Atmos., 114, 2009.

Lack, D. A., Cappa, C. D., Langridge, J., Bahreini, R., Buffaloe, G., Brock, C., Cerully, K., Coffman, D., Hayden, K., Holloway, J., et al.: Impact of Fuel Quality Regulation and Speed Reductions on Shipping Emissions: Implications for Climate and Air Quality, Environ. Sci. Technol., 45, 9052–9060, doi:10.1021/es2013424, 2011.

Lack, D. A. and Corbett, J. J.: Black carbon from ships: a review of the effects of ship speed, fuel quality and exhaust gas scrubbing, Atmos. Chem. Phys., 12, 3985-4000, doi:10.5194/acp-12-3985-2012, 2012.

Marelle, L., Thomas, J.L., Law, K.S., Raut, J.-C., Jalkanen, J.-P., Johansson, L., Roiger, A., Schlager, H., Kim, J., Reiter, A., Weinzierl, B., Rose, M.: Local and regional scale impacts of Arctic shipping emissions in northern Norway, to be submitted to ACP, 2015.

Moldanová, J., Fridell, E., Winnes, H., Holmin-Fridell, S., Boman, J., Jedynska, A., Tishkova, V., Demirdjian, B., Joulie, S., Bladt, H., Ivleva, N. P., and Niessner, R.: Physical and chemical characterisation of PM emissions from two ships operating in European Emission Control Areas, Atmos. Meas. Tech., 6, 3577-3596, doi:10.5194/amt-6-3577-2013, 2013.

Ødemark, K., Dalsøren, S. B., Samset, B. H., Berntsen, T. K., Fuglestvedt, J. S., and Myhre, G.: Short-lived climate forcers from current shipping and petroleum activities in the Arctic, Atmos. Chem. Phys., 12, 1979-1993, doi:10.5194/acp-12-1979-2012, 2012.

Petzold, A., Hasselbach, J., Lauer, P., Baumann, R., Franke, K., Gurk, C., Schlager, H., and Weingartner, E.: Experimental studies on particle emissions from cruising ship, their characteristic properties, transformation and atmospheric lifetime in the marine boundary layer, Atmos. Chem. Phys., 8, 2387-2403, doi:10.5194/acp-8-2387-2008, 2008.

Roiger, A. and Coauthors: Quantifying emerging local anthropogenic emissions in the Arctic region: the ACCESS aircraft campaign experiment, Bulletin of the American Meteorological Society, doi: 10.1175/BAMS-D-13-00169.1, 2014.

Song, C. H., Chen, G., Hanna, S. R., Crawford, J., and Davis, D. D.: Dispersion and chemical evolution of ship plumes in the marine boundary layer: Investigation of O3/NOy/HOx chemistry, J. Geophys. Res., 108, 4143, doi:10.1029/2002JD002216, D4, 2003.

Williams, E. J., Lerner, B. M., Murphy, P. C., Herndon, S. C. and Zahniser, M. S.: Emissions of NOx, SO2, CO, and HCHO from commercial marine shipping during Texas Air Quality Study (TexAQS) 2006, J. Geophys. Res., 114, D21306, doi:10.1029/2009JD012094, 2009.